

# Damage Detection Capabilities of Ultrasonic Phased Arrays and Sparse Arrays in Metallic and Composite Structures

M. SCHEERER, D. LAGER, M. MARISCHLER, F. GRAF  
and A. PELDSZUS

## ABSTRACT

In order to be able to inspect large areas of composite structures an ultrasonic SHM System based on Piezo-Actuators and Piezo-Sensors was developed where 8 actuators and 8 sensors are used to monitor 1 m<sup>2</sup> of a composite structure. Two different configurations were evaluated: a phased array configuration where the actuators and sensor were placed close to each other and a sparse array configuration where the actuators and sensors were spread over the area to be monitored. In both concepts each actuator was actuated by a burst signal confined in time and frequency and all sensors were used to capture the response of the structure before and after introduction of different damages. A delay and sum post processing algorithm where the difference between the individual signals before and after damage introduction were used as input was used to visualize the damaged region. The used algorithm also allows the compensation of environmental effects such as temperature. A lab based SHM system consisting of the piezo actuators and sensors, the actuation hardware and the control and data acquisition unit was set-up. The system and the post processing algorithm was tested on several panels made of Al and CFRP with different types of damages – holes and impact damages - between 300 and 800 mm<sup>2</sup> of overall size and both configurations – phased and sparse array - were compared regarding its damage detection, localization and quantification abilities.

## INTRODUCTION

Due to their contributions for weight reduction, the percentage of composite structural parts in commercial aircraft is continuously increasing. Still the full potential of the composite materials has not been reached, mainly due to uncertainties in the manufacturing process, the presence of barely visible impact damages (BVID's) and the prediction of the long term behaviour in use, leading to much higher safety factors compared to metals to date.

---

Michael Scheerer, AAC, c/o Forschungszentrum, 2444 Seibersdorf, (Austria), Email: michael.scheerer@aac-research.at



The effect of impact damages on the strengths of composite materials was studied intensively in the literature [1]. It was shown that impact damages of a size of 200 to 300 mm<sup>2</sup> in 3 mm CFRP panels (BVID's) lead to a reduction of approximately 30% of the compression strength.

If a non-destructive inspection system could be permanently applied to the structure of interest and operated online (Structural Health Monitoring), especially in distributed and difficult to access areas of composite structures, a strong reduction in the down time and subsequent costs of maintenance and also a reduction in weight with a further reduction of fuel consumption could be expected. Worldwide activities in the field of „Structural Health Monitoring” are continuously growing since more than two decades. An intensive overview of the various activities in the field of structural health monitoring can be found in “Health Monitoring of Aerospace Structures – Smart Sensor Technologies and Signal Processing” [2] and in the recently released “Encyclopedia of Structural Health Monitoring” [3]. It is possible to classify the different technologies by the used sensor principles or by the used SHM methodologies. The most promising sensor principles are based on piezoelectric materials, eddy current foils and fiber optic sensors like fiber Bragg grating sensors, extrinsic fabry perot interferometers or brillouin optical time domain reflectometry sensors. Analyses show that mainly the acoustic methods either passive as acoustic emission [4, 5] or active as lamb waves [6, 7] are able to cover larger areas with a sufficient size of detectable damage.

At the IWSHM2011 the authors have already presented the first results of such an active ultrasonic Phased Array SHM System based on Piezo-Actuators (PA) and Piezo Sensors (PS) and fibre optic sensors [8]. Out of these results more detailed analyses of the data with respect to the location of damages were required. Within this paper the authors present the latest developments of the system using two operational configurations for damage localization: phased array and sparse array. Both configurations have been tested to show their ability for the localization of damages such as holes and delaminations caused by impacts in flat panels made of Al and CFRP.

## **DESCRIPTION OF THE SYSTEM COMPONENTS**

In the above mentioned SHM concept a line array of 8 piezo actuators (PA) was actuated by a series of burst signals confined in time and frequency. The backscattered signals from potential defects in the structure were measured by 8 piezo sensors (PS). Depending on the placement of the sensors either as line array close to the actuators or spread over the area to be inspected two configurations have been realised – a phased array in the 1<sup>st</sup> and a sparse array in the 2<sup>nd</sup> configuration.

A lab based SHM system based on the mentioned technology consisting of the PA's with its actuation hardware, the PS's and the control and data acquisition unit was set-up. The system uses an arbitrary signal generator card ARB-1410-150 from MISTRAS (sampling rate: 125 MSamples/s, output voltage: 300 Vpp, frequencies of 700 kHz) for the actuation of one single PA. For data acquisition an oscilloscope card type Octopus<sup>TM</sup> OCT-848-002 from Gage Sensing that can measure up to 8 signals with 16 bit resolution and sampling rates up to 25 MS/s was used. Both cards were mounted in an external PCI box. For the control of the actuation electronic and for automated data acquisition a LabView program was implemented. The program has

the following features: full control of the waveform generator card, full control of the GaGe Octopus<sup>TM</sup>, setup of different actuator and sensor configurations and save data in ASCII and TDMS format (supplying correct meta-data). For both actuation and sensing arrays of smart layer<sup>TM</sup> actuators/sensors from Acellent have been used. All collected data were fed in a post processing algorithm described in the next paragraph.

### Post Processing of raw data

As the backscattered signals from defects are typically small compared to the reflections from the boundaries and the characteristic of the travelling lamb waves is complex no simple interpretation of the data taken only from a damaged structure is possible. Therefore the acoustic response of the structure (collected signals from all sensors for all active actuators) will be measured before (baseline measurement) and after the appearance of damages and compared against each other. The comparison was done by a subtraction of the individual transient signals before and after the occurrence of the damage. The difference signals are the basis for damage detection, localization and quantification. Therefore any change in the transient signals between the baseline measurement and the measurement after the occurrence of damage beside that caused by the damage itself could lead to misinterpretations. Figure 1 illustrates the effect of the temperature on the measured signal at a distance of 150 mm from an actuator actuated by 3 sin burst with a centre frequency of 60 kHz.

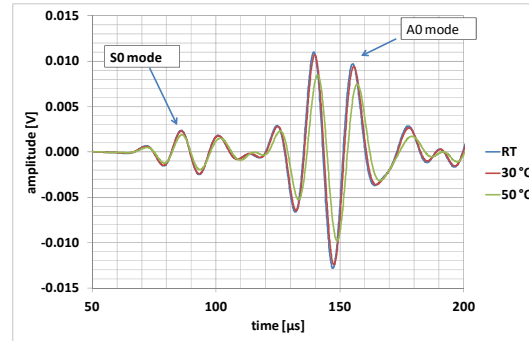


Figure 1. Measured transient signals from a piezo sensor at 150 mm distance from the piezo actuator at different temperatures.

When comparing the measurements at different temperatures the following conclusions can be drawn: the higher the temperature difference, the larger the difference between the two signals; the wave velocities and the damping of the travelling lamb waves change with temperature – the higher the temperature, the lower the wave velocity and the higher the damping (see Figure 1) and the effect is larger when the actuation frequency is higher. The average wave velocity change / temperature is in the range of 1.7 (m/s)/K for the A0 mode at 60 kHz and 0.22 (m/s)/K for the S0 mode at 250 kHz. The influences seem to be low but produce remarkable difference signals if the signals will be subtracted from each other. Therefore the influence of the environment and especially the temperature that lead to changes in the amplitude and wave speed are critical and need to be minimized to reduce their influences on the results. The following steps were used in the post processing algorithm. In a 1<sup>st</sup> step the raw data from all piezo sensors were filtered using an FIR (or respectively FFT) band pass filter to remove the noise and direct current content.

In a 2<sup>nd</sup> step the filtered signals coming from two different measurements – baseline measurement and measurement after the introduction of the impact are compared to each other in order to compensate environmental effects. The maximum measured amplitudes of the individual filtered signal will be normalized to a value of 1. In a 3<sup>rd</sup> step the frequency response of the individual signals will be compared and the frequency spectrum of the measurement after the damage will be shifted to higher or lower frequencies to achieve a minimum standard deviation with respect to the baseline measurement. This frequency shift algorithm aims to compensate differences in propagation speed. The 4<sup>th</sup> step is used to visualize the results by transferring the filtered and corrected transient signals from the time domain to the 2-dimensional space domain. Therefore a near-field beam forming algorithm was used. The algorithm is based on the time-of-flight principle. First part is to define a mesh of planar coordinates (x, y) over the plate. For each position the distance to the corresponding actuator  $I_{aj}(x, y)$  and sensor  $I_{sj}(x, y)$  is calculated. Assuming a fixed propagation speed  $c$  the distances are transformed into time delays  $(t_{sj}(x, y)_c / t_{aj}(x, y)_c)$ . With the known central time of actuation the corresponding time of observation  $t_{obs}$ , where a reflection would be observed for the coordinates  $x$  and  $y$ , is calculated by  $t_{obs} = t_{offset} + t_{sj}(x, y)_c + t_{aj}(x, y)_c$ . For each combination of sensors and actuators and each position the time of observation is calculated. A time window with time dilation of the corresponding wavelet is centred around  $t_{obs}$ . This signal window is windowed by a hamming window to smooth the signal. These windows, which inherently contain the near-field steering delays for both actuation and sensing arrays, are simply added. In this step the delay-and-sum beam forming applies. Hence for each position a beam formed signal window is obtained, which is used to calculate the squared power sum, breaking down the signal vector into a scalar, which gives information about the reflectivity at this position.

## RESULTS OF VALIDATION TESTS

In order to validate the developed system, tests on an Al-plate (800 x 400 x 5 mm<sup>3</sup>) and a quasi-isotropic CFRP plate [0/90/-45/45]<sub>2s</sub> (790 x 400 x 4.8 mm<sup>3</sup>) have been performed. The used material for the CFRP plate is a Cytec 977-2A-42%-6KHTA-2x2TW-285. The actuation array was placed on the long side of the test article at a distance of approximately  $\lambda/2$  from the boundary in order to allow constructive interference of the reflected beam. The PS sensor arrays were either placed direct in front of the actuator array in case of the phased array configuration and along the remaining three edges in case of the sparse array configuration as illustrated in figure 2. In the Al plate 2 damages have been introduced: a 20 mm hole and later a 20 x 40 mm long hole. In the CFRP plate two impacts one with 10 J (overall damage area: 300 mm<sup>2</sup>), a second impact with 15 J (overall damage area: 670 mm<sup>2</sup>) and later a 20 mm hole have been introduced. For actuation of the PA's a Morlet type Wavelet with two different centre frequencies was used. All measurements have been repeated 10 times at three different days for each state of the structure (undamaged and damaged) in order to evaluate the reproducibility of the results.

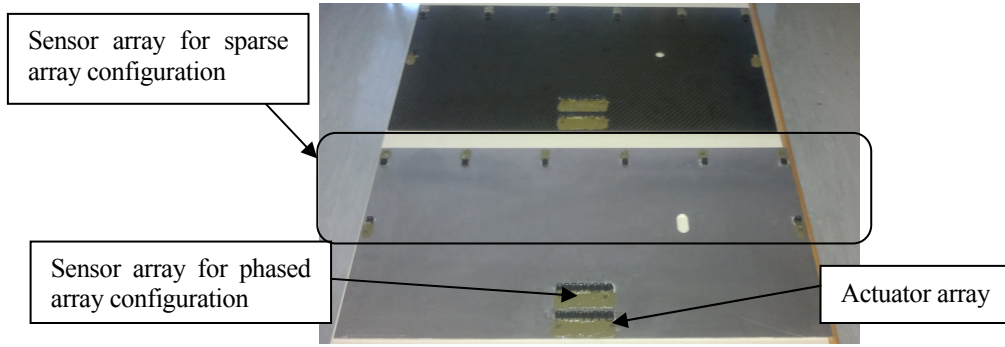


Figure 2. Al and CFRP plate with mounted actuator and sensor arrays for phased array and sparse array configurations.

The following table shows the used pseudo-frequencies, the wave velocities of the present lamb wave modes and the present wavelength for both materials. The required group velocities have been derived from the program “DISPERSE” and verified by wave propagation measurements at selected frequencies. In Table I the bold marked fields indicate the preferred operating regimes for the used array configuration: distance of the PA’s is close to  $\lambda/2$ .

Table I. pseudo-frequencies, Group velocities and wavelength for both materials.

f [kHz]	Al plate (5mm)				CFRP Plate (4.8 mm)			
	A0		S0		A0		S0	
	$v_g$ [m/s]	$\lambda$ [mm]	$v_g$ [m/s]	$\lambda$ [mm]	$v_g$ [m/s]	$\lambda$ [mm]	$v_g$ [m/s]	$\lambda$ [mm]
<b>60</b>	<b>2600</b>	<b>43.3</b>	5430	90.5	<b>1534</b>	<b>25.6</b>	5430	91.3
<b>250</b>	3166	12.7	<b>4900</b>	<b>19.60</b>	1540	5.3	<b>5230</b>	<b>20.9</b>

### Test on the AL Plate

For testing of the Al plate the used wave velocities selected for data evaluation were 2600 m/s for the 60 kHz actuation corresponding to the A0 mode and 4900 m/s for the 250 kHz actuation corresponding to the S0 mode. Figure 3 illustrated the results achieved on the Al panel damaged by a 20 mm hole using 60 kHz and 250 kHz for actuation in phased array and in sparse array configurations.

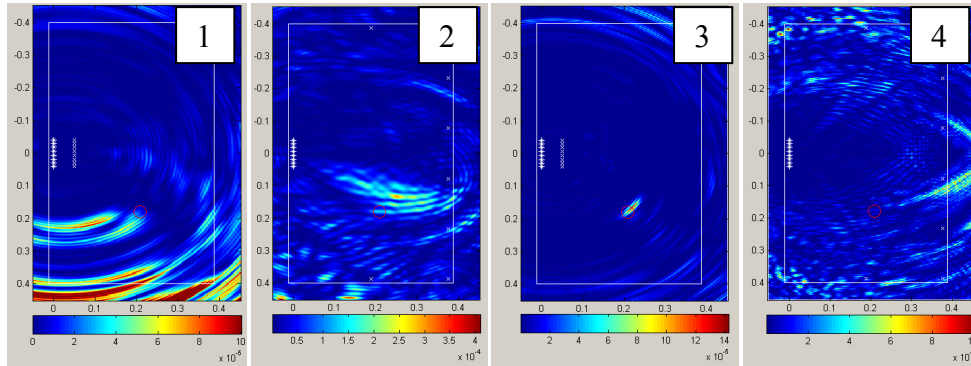


Figure 3. results achieved on the Al panel damaged by a 20 mm hole using 60 kHz in phased array (1) and sparse array (2) and 250 kHz in in phased array (3) and in sparse array configuration (4).

The best localization of the 20 mm hole was achieved using an actuation frequency of 250 kHz in phased array configuration. The second best result was achieved for a 60 kHz actuation in sparse array configuration. In both other cases the position of the maximum residuum does not appear close to the region of the defect especially in case of the sparse array configuration using 250 kHz for actuation. For the best configuration (phased array with an actuation frequency of 250 kHz) the second damage (20 x 40 mm<sup>2</sup> long hole) was analyzed to assess the possibility for damage size quantification as shown in figure 4. It can be demonstrated the maximum residuum scales with damage size. The value for zero damage has been taken out of the highest residuum of the repeated measurements at the individual stages (noise of the measurement campaign).

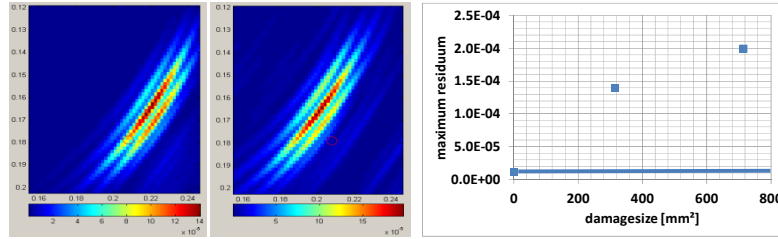


Figure 4. maximum residuum as function of the damage size using the phased array configuration and an actuation frequency of 250 kHz.

### Test on CFRP Plate

The used wave velocities selected for data evaluation in the CFRP panel were 1530 m/s for the 60 kHz actuation corresponding to the A0 mode and 5230 m/s for the 250 kHz actuation corresponding to the S0 mode.

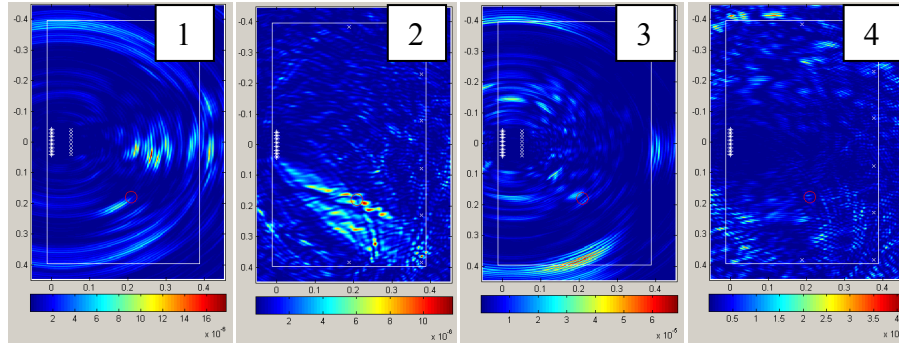


Figure 5. Results achieved on the CFRP panel damaged by 20 mm using 60 kHz in phased array (1) and sparse array (2) and 250 kHz in phased array (3) and in sparse array configuration (4).

Figure 5 illustrated the results achieved on the CFRP panel damaged by a 20 mm hole using 60 kHz and 250 kHz for actuation in phased array and in sparse array configurations. In general the damping of the signals was remarkable higher compared to the Al plate. Similar localization errors as for the Al plate have been found when analyzing the data for an actuation at 60 kHz in phased array configuration and an actuation at 250 kHz in sparse array configuration. Contrary to the Al panel the best results have been achieved for the actuation at 60 kHz in sparse array configuration. For both frequencies in phased array configuration there is an indication of the impact damage but several other echoes appear over the panel. The reason for the appearance



of ghost echoes can be explained by the propagation of different modes within the panel. Although the dominant modes at the two different frequencies have been used to detect the damage the second mode is present. Especially in case of the actuation with 60 KHz where the slow A0 mode is dominant also the much quicker S0 mode eventually interact with the defect and with the boundaries leading to the observed ghost reflections. In addition so far only the dominant mode was used in the algorithm to locate the damage. A phenomenon is the effect mode conversion where e.g. the S0 mode arriving at the damage stimulates the reflection and scatter of the A0 mode. In order to validate the assumption above two different wave speeds 1 from the actuator to the potential damage and a second from this damage to the sensor has been used to study the effect of mode conversion and secondly tacky tapes to limit reflections from the edges were placed at the edges of the panel in an additional test campaign. The two left images of figure 6 illustrate the effect of mode conversion whereas the two right images illustrate the effect of tacky tapes for both actuation frequencies in phased array configuration.

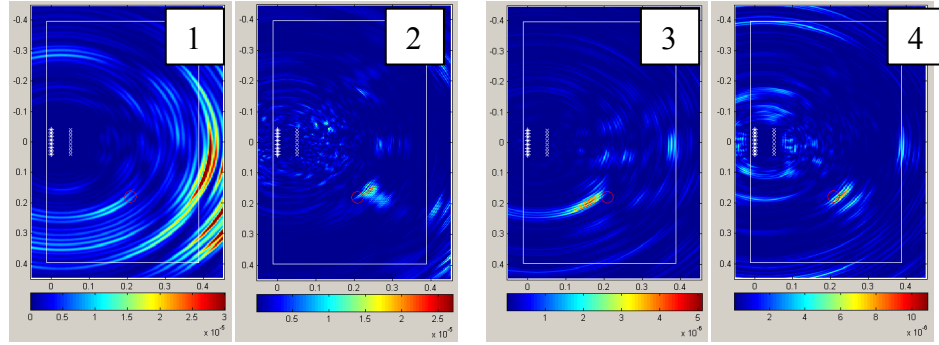


Figure 6. Effect of mode conversion for 60 KHz (1) and 250 KHz (2) and effect of tacky tapes for 60 KHz (3) and 250 KHz (4) in phased array configuration.

When analyzing the effect of mode conversion the larger effect is coming from the conversion from the S0 mode at 250 KHz to A0 mode illustrated as a large residuum at the position of the defect in image 2 of figure 6. The reduction of the reflections when using tacky tapes clearly demonstrated the influences of the reflection on the proper location of the damage especially in phased array configuration. The 20 mm hole can be clearly located for both actuation frequencies in phased array configuration.

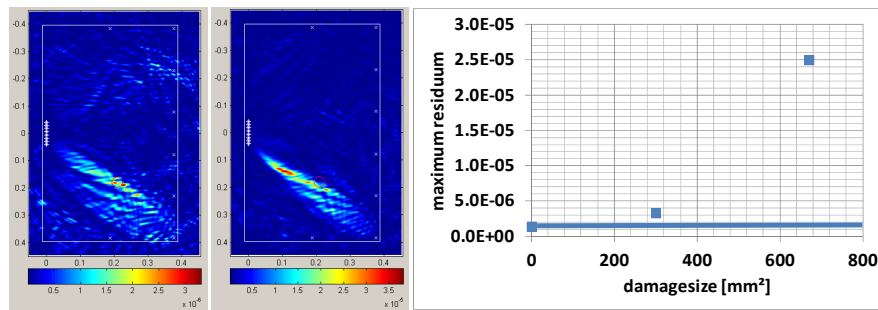


Figure 7. Impact damage detection with 60 KHz in sparse array configuration without tacky tape (left: damage size: 300 mm², middle: damage size 670 mm², right: residuum vs. damage size).

For the best configuration – using an actuation frequency of 60 kHz in sparse array configuration – the results for the two different impact damages has been analyzed as shown in figure 7. It was demonstrated that the maximum residuum close to the damage position scales with the damage size similar to the findings in the Al plate.

## SUMMARY

Two different configuration of imaging techniques for guided ultrasonic waves – phased array and sparse array – have been analyzed regarding the ability for localization and quantification of different damage in Al and CFRP panels.

It was shown that effect of reflections from boundaries has large influences in the proper localization of damages especially in the CFRP plate. In cases where the boundaries are far away from the damage phased array configurations are favourable whereas in the other case sparse array configurations where the sensors are placed close to the boundaries show better results.

Using the phased array configuration and a dominant S0 mode at 250 kHz all damages could be detected, localized and quantified in the Al plate. Using the sparse array configuration and a dominant A0 mode at 60 kHz all impact damages could be detected, localized and quantified in the CFRP plate but with less accuracy compared to the Al plate.

## ACKNOWLEDGEMENT

The presented work has been funded by the Austrian Promotion Agency within the Take Off projects ASHMOSD-I and ASHMOSD-II which is gratefully acknowledged.

## REFERENCES

1. Herzsberg, 1999. An engineering approach for predicting residual strength of carbon/epoxy laminates after impact and hygrothermal cycling. *Composite Structures* 47 (1999) 483-490.
2. W.J. Staszekski, C. Boller, G.R. Tomlinson, 2004. *Health Monitoring of Aerospace Structures – Smart Sensor Technologies and Signal Processing*. John Wiley & Sons Ltd. ISBN 0-470-84340-3.
3. Christian Boller, Fu-Kou Chang, Yozo Fujino, 2009. *Encyclopedia of Structural Health Monitoring*. John Wiley & Sons Ltd. ISBN 978-0-470-05822-0.
4. Christophe A. Paget, Kathryn Atherton and Eddie O'Brien, 2004. Damage Assessment in a Full-Scale Aircraft Wing by Modified Acoustic Emission. *Proc. of 2<sup>nd</sup> EWSHM*.
5. M. Scheerer, T. Goss, M. Henzel, M. Marischler, R. Wagner, 2010. Impact Damage Quantification by Analyses of Acoustic Emission Data. *Proc. 14th ECCM*, June 7-10 2010, Budapest, Hungary.
6. V. Giurgiutiu, 2008. *Structural Health Monitoring with Piezoelectric waver active sensors*. Academic Press, ISBN 978-0-12-088760-6, 2008.
7. Improvement of Damage Detection with the Embedded Ultrasonics Structural Radar for Structural Health Monitoring; Lingyu Yu, Giurgiutiu Victor, University of South Carolina; *Proc. of 5th Int. Workshop on Structural Health Monitoring* (2005).
8. M. Scheerer, C. Bockenheimer, A. Dantele, Z. Djinicovic, F. Graf, T. Natschläger, A. Peldszus, M. Reiterer, T. Sauter, R. Stössel.: Development and testing of an ultrasonic phased array system based on piezo actuators and fiber optic sensors, *Proc. 8th IWSHM*, Stanford, US (2011), pp. 967 – 974.